Hyperfine quenching of the $1s^2 2s2p\,{}^3P_0$ level in berylliumlike ions

J. P. Marques and F. Parente

Centro de Física Atómica Instituto National de Investigação Científica e Departamento de Física da Universidade de Lisboa, Avenida Gama Pinto 2, P-1699 Lisboa Codex, Portugal

P. Indelicato

Laboratoire de Physique Atomique et Nucléaire, Boîte 93, Université Pierre et Marie Curie, 4 place Jussieu, F-75252 Paris CEDEX 05, France

(Received 13 May 1992)

In this paper, we used the multiconfiguration Dirac-Fock method to compute with high precision the $1s^2 2s2p\,{}^3P_1$–$1s^2 2s2p\,{}^3P_0$ separation energy in berylliumlike ions, including the relativistic contribution to electron-electron correlations and radiative corrections. The effect of the hyperfine interaction on both the energy and lifetimes of those levels has been evaluated. In the absence of nuclear magnetic moment the ${}^3P_0$ level can decay to the ground state only by an $E1$-$M1$ transition, with a very low probability. We show that the hyperfine interaction increases dramatically the ${}^3P_0$ transition probability.

PACS number(s): 31.30.Gs,31.30.Jv,32.70.Fw

I. INTRODUCTION

It has been found before, both theoretically and experimentally, that the hyperfine interaction plays a fundamental role in the lifetimes and energy separations of $1s2p\ {}^3P_0$ and $1s2p\ {}^3P_1$ levels in heliumlike ions [1–3]. In those systems, in the region $Z \approx 45$, these two levels undergo a level crossing [4] and are nearly degenerate because of magnetic interaction, which leads to the strong influence of the hyperfine interaction on the energy splitting and on the $2\ {}^3P_0$ lifetime for isotopes with nonzero nuclear spin.

In this paper we extend our previous calculations to the influence of the hyperfine interaction on the $1s^2 2s2p$ levels in berylliumlike ions. The energy level diagram for berylliumlike Xe is shown in Fig. 1. In these systems a level crossing of the ${}^3P_0$ and ${}^3P_1$ levels has not been found. One-photon transitions from the $2\ {}^3P_0$ to the ground state are forbidden, multiphoton transitions have been found to be negligible, and therefore the lifetime of this level may be considered infinite to a very good approximation. The energy separation between $2\ {}^3P_0$ and $2\ {}^3P_1$ levels is very small for low values of Z and increases very rapidly with Z. However, hyperfine interaction still has a strong influence on the energy splitting and on the $2\ {}^3P_0$ lifetime for isotopes with nonzero nuclear spin. On the other hand, the ${}^3P_2$ level is very close to the ${}^3P_0$ and ${}^3P_1$ levels for low values of Z.

The different steps of this calculation are described in Refs. [1,5]. Here we will emphasize only the fundamental topics of the theory and the characteristic features of berylliumlike systems.

The multiconfiguration Dirac-Fock method [6, 7] (MCDF) is used to evaluate the $1s^2 2s2p$ fine-structure separation $\Delta E_{0;\mathrm{FS}} = E_{{}^3P_1} - E_{{}^3P_0}$. Several terms, such as the nonrelativistic contribution to the correlation, are the same for both levels. In this paper we calculate residual terms, including Breit interaction, one-particle self-energy and vacuum polarization, and two-electron radiative corrections using the method described in [1, 6–8]. The MCDF method, in principle, allows for precise calculations, because it can include most of the correlation relatively easily, i.e., with a small number of configurations. Here correlation is important in the determination of transition energies to the ground state, which are used in the calculation of transition probabilities. The largest effect is obtained by using $1s^2 2s^2$, $1s^2 2p_{1/2}^2$, and $1s^2 2p_{3/2}^2$ as the configuration set for the ground state. For the $1s^2 2s2p\ {}^3P_J$ energy, no correlation was included because it has a very small contribution to the transition probability, and because $\Delta E_{0;\mathrm{FS}}$, which is

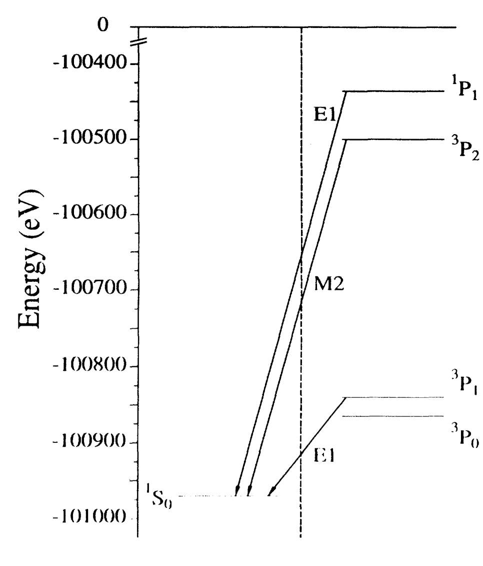

FIG. 1. Energy level and transitions diagram for berylliumlike xenon ($Z = 54$).

the important parameter in the calculation of the hyperfine quenching, is not very sensitive to correlation: the main contribution to the correlation in that case is the nonrelativistic contribution, which is J invariant in the nonrelativistic case. Because of the preceding considerations, we have used respectively only three configuration state functions (CSF) ($|1s^22s^2\ J=0\rangle$, $|1s^22p_{1/2}^2\ J=0\rangle$, and $|1s^22p_{3/2}^2\ J=0\rangle$) for the ground state and only one CSF ($|1s^22s2p_{1/2}\ J=0\rangle$), and two ($|1s^22s2p_{1/2}\ J=1\rangle$, ($|1s^22s2p_{3/2}\ J=1\rangle$) for the excited states. The same set of CSF have been used for energy, transition probabilities, and for hyperfine matrix elements calculations. In our previous work on a heliumlike system we had also used single CSF for transition probabilities and hyperfine matrix elements calculations, but we did a very complete calculation of correlation energy for all three levels $1s^2$ and $1s2p\ {}^3P_J$. This calculation has shown us that correlation contribution to the fine-structure separation $\Delta E_{0;\mathrm{FS}}$ was very small indeed. There are very recent calculations of correlation in $1s^22s2p\ {}^3P_1 \rightarrow 1s^22s^2\ {}^1S_0$ transitions in Fe and Mo [9], using relativistic many-body perturbation theory. Still, no evaluation of $\Delta E_{0;\mathrm{FS}}$ has been done in Ref. [9] that we could use to test more precisely the accuracy of our calculation.

Finally we would like to point out that all energy calculations are done in the Coulomb gauge for the retarded part of the electron-electron interaction, to avoid spurious contributions (see, for example, Refs. [8, 10]). The lifetime calculations are all done using exact relativistic formulas. The length gauge has been used for all transition probabilities.

II. RELATIVISTIC CALCULATION OF HYPERFINE CONTRIBUTION TO FINE-STRUCTURE SPLITTING AND TO TRANSITION PROBABILITIES

In the case of a nucleus with nonzero spin, the hyperfine interaction between the nucleus and the electrons must be taken into account. The correspondent Hamiltonian can be written as

$$H_{\mathrm{HFS}} = \sum_k \mathbf{M}^{(k)}\cdot\mathbf{T}^{(k)}, \tag{2.1}$$

where $\mathbf{M}^{(k)}$ and $\mathbf{T}^{(k)}$ are spherical tensors of rank k, representing, respectively, the nuclear and the atomic parts of the interaction. As in the case of heliumlike ions, the only sizable contribution from Eq. (2.1) is the magnetic dipole term ($k=1$). The contribution of this interaction for the total energy has been evaluated through the diagonalization of the following matrix, for $F=\frac{1}{2}$:

$$H_{\mathrm{tot}} = \begin{bmatrix} E_1 + \frac{1}{2}i\Gamma_1 + W(1,1) & W(1,2) & W(1,3) \\ W(2,1) & E_2 + \frac{1}{2}i\Gamma_2 + W(2,2) & W(2,3) \\ W(3,1) & W(3,2) & E_3 + \frac{1}{2}i\Gamma_3 + W(3,3) \end{bmatrix}. \tag{2.2}$$

Here, E_f is the unperturbed level energy and Γ_f is the radiative width of the unperturbed level ($f=1$–3 stands, respectively, for ${}^3P_0, {}^3P_1, {}^1P_1$). A similar matrix must be diagonalized, for $F=\frac{3}{2}$, with the ${}^3P_0$ level replaced by ${}^3P_2$. $W(f,f') = \langle 1s^22s2p\ f|H_{\mathrm{HFS}}|1s^22s2p\ f'\rangle$ is the unperturbed hyperfine matrix element. This quantity may be written as

$$W(J_1,J_2) = \langle I,J_1,F,M_F|\mathbf{M}^{(1)}\cdot\mathbf{T}^{(1)}|I,J_2,F,M_F\rangle, \tag{2.3}$$

where I is the nuclear spin and F the total angular momentum of the atom, and may be set in the form

$$W(J_1,J_2) = (-1)^{I+J_1+F}\begin{Bmatrix} I & J_1 & F \\ J_2 & I & 1 \end{Bmatrix} \times \langle I||\mathbf{M}^{(1)}||I\rangle\langle J_1||\mathbf{T}^{(1)}||J_2\rangle. \tag{2.4}$$

The $6j$ symbol leads to $W(0,0)=0$. Also the nuclear magnetic moment μ_I in units of the nuclear magneton μ_N may be defined by

$$\mu_I\mu_N = \langle I||\mathbf{M}^{(1)}||I\rangle \begin{pmatrix} I & 1 & I \\ -I & 0 & I \end{pmatrix}, \tag{2.5}$$

with $\mu_N = e\hbar/(m_pc)$.

The electronic matrix elements were evaluated on the basis set

$$|{}^3P_0\rangle, |{}^3P_1\rangle, |{}^1P_1\rangle, |{}^3P_2\rangle$$

with

$$\begin{aligned} |{}^3P_0\rangle &= |1s^22s2p_{1/2}\ J=0\rangle, \\ |{}^3P_1\rangle &= \alpha|1s^22s2p_{1/2}\ J=1\rangle + \beta|1s^22s2p_{3/2}\ J=1\rangle, \\ |{}^1P_1\rangle &= \beta|1s^22s2p_{1/2}\ J=1\rangle - \alpha|1s^22s2p_{3/2}\ J=1\rangle, \\ |{}^3P_2\rangle &= |1s^22s2p_{3/2}\ J=2\rangle. \end{aligned}$$

Electron correlation was neglected in the evaluation of matrix elements because its effect is small compared to available experimental precision. Upon diagonalization of the total energies matrix (2.2) for $F=\frac{1}{2}$ and $F=\frac{3}{2}$, for a few values of Z, we found that the influence of the ${}^1P_1$ and ${}^3P_2$ levels on the lifetimes of the ${}^3P_0$ and ${}^3P_1$ is negligible; therefore, instead of the matrix (2.2) we limited ourselves to the following smaller matrix, replacing ${}^3P_0$ by 0 and ${}^3P_1$ by 1:

$$H_{\mathrm{tot}} = \begin{bmatrix} E_0 + \frac{1}{2}i\Gamma_0 + W(0,0) & W(1,0) \\ W(0,1) & E_1 + \frac{1}{2}i\Gamma_1 + W(1,1) \end{bmatrix}. \tag{2.6}$$

The final result is then obtained by a diagonalization of the 2×2 matrix in Eq. (2.6), the real part of each eigenvalue being the energy of the correspondent level and the imaginary part its lifetime.

III. RESULTS AND DISCUSSION

The method outlined in Sec. II has been used to evaluate the influence of the hyperfine interaction on both the $1s^22s2p\ ^3P_0$ and $^3P_1$ levels for all Z between 5 and 92 and for all stable and some quasistable isotopes of nonzero spin. Terms coming from higher multipoles have been found to be negligible.

A detailed list of the contributions to the theoretical $1s^22s2p\ ^3P_0$ and $^3P_1$ level energies is presented in Table I for $Z = 6, 36, 54, 82$. In Table II we present, for all possible values of the nuclear spin I, as a function of Z, the unperturbed separation energies ΔE_0, the diagonal and off-diagonal hyperfine matrix elements $W(1,1)$ and $W(1,0)$, the magnetic dipole moments [11] μ_i, and the separation energies $\Delta E_{\rm HF}$ which are the difference of the eigenvalues of Eq. (2.6). In Fig. 2 is plotted the difference of $E = \Delta E_{\rm HF} - \Delta E_0$ for the different nuclear spins. The influence of the hyperfine interaction on this energy is shown to increase slowly with Z.

In Table III we present, for all possible values of the nuclear spin I, as a function of Z, the perturbed $1s^22s2p\ ^3P_0$ lifetime τ_0 (the unperturbed τ_0 is infinite in first approximation) and the $1s^22s2p\ ^3P_1$ lifetime τ_1 which is not affected, within the precision shown by the hyperfine interaction. In Fig. 3 is plotted the perturbed $1s^22s2p\ ^3P_0$ lifetime for the different nuclear spins I, as a function of Z. One can see that the opening of a new channel for the decay of the $1s^22s2p\ ^3P_0$ has a dramatic effect on its lifetime. This can be seen in the case of lead, for example. Using our transition probability code, we made a rough estimate of the $E1$-$M1$ transition rate. We included only the first few excited states and neglected possible resonant structure. The integrated rate we have obtained is

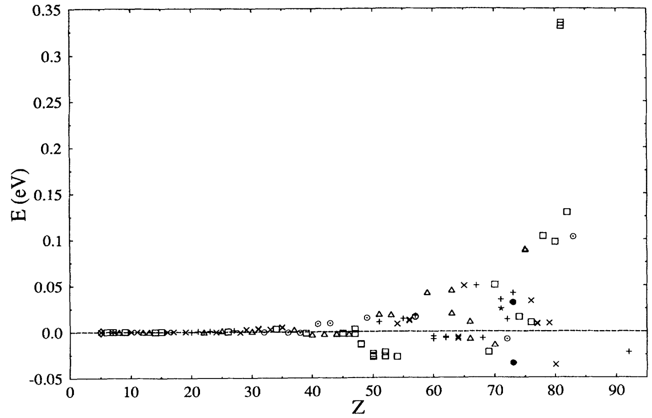

FIG. 2. Influence of the hyperfine interaction on the $1s^22s2p\ ^3P_1 - 1s^22s2p\ ^3P_0$ energy separation, as a function of the nuclear spin I and the atomic number Z. The quantity $E = \Delta E_{\rm HF,I} - \Delta E_0$ is the contribution of the hyperfine interaction to the fine-structure splitting ΔE_0. The symbols $\square$, $\times$, $\triangle$, $+$, $\odot$, $*$, $\diamond$, $\circ$, $\star$, and $\bullet$ represent values for isotope with nuclear spin I of $\frac{1}{2}$, $\frac{3}{2}$, $\frac{5}{2}$, $\frac{7}{2}$, $\frac{9}{2}$, 1, 3, 5, 7, and 9, respectively. Some elements have several isotopes with identical spins but different μ_i.

TABLE I. Contribution to the energy of the $1s^22s2p\ ^3P_1$ and $1s^22s2p\ ^3P_0$ levels ($Z = 6, 36, 54, 82$) and to the fine-structure separation ΔE_0. All energies are in eV.

	$^3P_1$	$^3P_0$	ΔE_0	$^3P_1$	$^3P_0$	ΔE_0
		$Z = 6$			$Z = 36$	
Coulomb energy	-986.418	-986.422	0.004	-43283.963	-43295.035	11.071
Magnetic energy	0.075	0.076	-0.001	21.956	22.495	-0.539
Lowest-order retardation ($\Delta\omega^2$)	-0.001	-0.001	0.000	-0.756	-0.755	0.000
High-order retardation ($\Delta\omega^n, n > 2$)	0.000	0.000	0.000	-0.003	0.001	-0.004
Self-energy	0.054	0.054	0.000	27.576	27.564	0.012
Self-energy screening	-0.007	-0.007	0.000	-0.750	-0.744	-0.005
Vacuum polarization $\alpha(Z\alpha)$	-0.002	-0.002	0.000	-2.816	-2.816	0.001
Vacuum polarization $\alpha(Z\alpha)^3$	0.000	0.000	0.000	0.032	0.032	0.000
Vacuum polarization $\alpha^2(Z\alpha)$	0.000	0.000	0.000	-0.023	-0.023	0.000
Total energy	-986.300	-986.303	0.003	-43238.747	-43249.282	10.535
		$Z = 54$			$Z = 82$	
Coulomb energy	-101009.779	-101034.668	24.889	-250750.523	-250795.364	44.841
Magnetic energy	78.288	79.965	-1.677	302.464	309.802	-7.338
Lowest-order retardation ($\Delta\omega^2$)	-2.727	-2.725	-0.002	-10.271	-10.268	-0.003
High-order retardation ($\Delta\omega^n, n > 2$)	0.012	0.016	-0.004	0.374	0.375	-0.001
Self-energy	109.782	109.776	0.007	494.333	494.332	0.001
Self-energy screening	-2.200	-2.174	-0.026	-8.225	-8.123	-0.102
Vacuum polarization $\alpha(Z\alpha)$	-15.418	-15.421	0.004	-109.010	-109.032	0.022
Vacuum polarization $\alpha(Z\alpha)^3$	0.347	0.347	0.000	4.608	4.609	-0.001
Vacuum polarization $\alpha^2(Z\alpha)$	-0.122	-0.122	0.000	-0.840	-0.841	0.000
Total energy	-100841.815	-100865.006	23.191	-250077.090	-250114.509	37.419

TABLE II. Influence of the hyperfine interaction on the $1s^22s2p\ ^3P_1 - 1s^22s2p\ ^3P_0$ energy separation, as a function of the nuclear spin I and the atomic number Z. The unperturbed energy separation is ΔE_0 (eV) and $\Delta E_{\rm HF}$ (eV) is the energy when the hyperfine interaction is taken into account. The hyperfine matrix elements $W(1,0)$ and $W(1,1)$ from Eq. (2.6) are given in eV and the nuclear magnetic moment μ_i is given in nuclear magneton units.

I	Z	A	ΔE_0	$\Delta E_{\rm HF}$	$W(1,0)$	$W(1,1)$	μ_i
$\frac{1}{2}$	6	13	0.003	0.003	-4.708×10^{-06}	6.044×10^{-06}	0.7024118
	7	15	0.008	0.008	3.384×10^{-06}	-4.563×10^{-06}	-0.283188842
	9	19	0.032	0.032	-7.700×10^{-05}	1.105×10^{-04}	2.628868
	14	29	0.289	0.289	7.322×10^{-05}	-1.148×10^{-04}	-0.55529
	15	31	0.397	0.398	-1.882×10^{-04}	2.995×10^{-04}	1.13160
	26	57	3.862	3.863	-9.926×10^{-05}	1.868×10^{-04}	0.09044
	34	77	9.060	9.063	-1.533×10^{-03}	3.181×10^{-03}	0.5350422
	39	89	12.775	12.774	6.466×10^{-04}	-1.389×10^{-03}	-0.13741542
	45	103	17.160	17.159	7.006×10^{-04}	-1.540×10^{-03}	-0.08840
	47	107	18.563	18.561	1.057×10^{-03}	-2.334×10^{-03}	-0.113570
	47	109	18.563	18.566	-1.215×10^{-03}	2.683×10^{-03}	0.130563
	48	111	19.251	19.238	5.986×10^{-03}	-1.324×10^{-02}	-0.59488607
	48	113	19.251	19.237	6.262×10^{-03}	-1.385×10^{-02}	-0.62230092
	50	115	20.601	20.577	1.077×10^{-02}	-2.390×10^{-02}	-0.91883
	50	117	20.601	20.575	1.174×10^{-02}	-2.604×10^{-02}	-1.00104
	50	119	20.601	20.573	1.228×10^{-02}	-2.725×10^{-02}	-1.04728
	52	123	21.914	21.891	1.002×10^{-02}	-2.229×10^{-02}	-0.7369478
	52	125	21.914	21.887	1.208×10^{-02}	-2.687×10^{-02}	-0.88850513
	54	129	23.191	23.164	1.222×10^{-02}	-2.724×10^{-02}	-0.7779763
	69	169	31.681	31.658	9.887×10^{-03}	-2.225×10^{-02}	-0.2316
	70	171	32.179	32.230	-2.244×10^{-02}	5.054×10^{-02}	0.49367
	74	183	34.085	34.101	-6.875×10^{-03}	1.553×10^{-02}	0.11778476
	76	187	34.982	34.992	-4.274×10^{-03}	9.673×10^{-03}	0.06465189
	78	195	35.838	35.942	-4.559×10^{-02}	1.034×10^{-01}	0.60952
	80	199	36.652	36.749	-4.279×10^{-02}	9.731×10^{-02}	0.50588549
	81	203	37.041	37.373	-1.459×10^{-01}	3.324×10^{-01}	1.62225787
	81	205	37.041	37.376	-1.474×10^{-01}	3.356×10^{-01}	1.63821461
	82	207	37.419	37.548	-5.669×10^{-02}	1.293×10^{-01}	0.592583
$\frac{3}{2}$	5	11	0.001	0.001	-6.498×10^{-06}	3.461×10^{-06}	2.6886489
	10	21	0.056	0.056	2.080×10^{-05}	-1.365×10^{-05}	-0.661797
	11	23	0.090	0.090	-9.654×10^{-05}	6.457×10^{-05}	2.2175219
	16	33	0.532	0.532	-9.915×10^{-05}	7.161×10^{-05}	0.6438212
	17	35	0.696	0.696	-1.553×10^{-04}	1.138×10^{-04}	0.8218743
	17	37	0.696	0.696	-1.293×10^{-04}	9.473×10^{-05}	0.6841236
	19	39	1.125	1.125	-1.079×10^{-04}	8.145×10^{-05}	0.39146616
	19	41	1.125	1.125	-5.920×10^{-05}	4.470×10^{-05}	0.21487009
	24	53	2.876	2.876	2.929×10^{-04}	-2.391×10^{-04}	-0.47454
	28	61	4.999	4.998	7.984×10^{-04}	-6.914×10^{-04}	-0.75002
	29	63	5.616	5.618	-2.687×10^{-03}	2.359×10^{-03}	2.2273456
	29	65	5.616	5.619	-2.873×10^{-03}	2.522×10^{-03}	2.38161
	31	69	6.934	6.936	-3.090×10^{-03}	2.780×10^{-03}	2.016589
	31	71	6.934	6.937	-3.926×10^{-03}	3.532×10^{-03}	2.562266
	33	75	8.336	8.338	-2.761×10^{-03}	2.538×10^{-03}	1.439475
	35	79	9.794	9.798	-4.996×10^{-03}	4.675×10^{-03}	2.106400
	35	81	9.794	9.799	-5.385×10^{-03}	5.039×10^{-03}	2.270562
	54	131	23.191	23.199	-8.099×10^{-03}	8.075×10^{-03}	0.6918619
	56	135	24.433	24.444	-1.130×10^{-02}	1.128×10^{-02}	0.837943
	56	137	24.433	24.445	-1.264×10^{-02}	1.262×10^{-02}	0.937365
	64	155	29.059	29.054	5.937×10^{-03}	-5.957×10^{-03}	-0.25723
	64	157	29.059	29.052	7.784×10^{-03}	-7.811×10^{-03}	-0.33726
	65	159	29.600	29.650	-4.961×10^{-02}	4.980×10^{-02}	2.014
	76	189	34.982	35.015	-3.252×10^{-02}	3.291×10^{-02}	0.659933
	77	191	35.415	35.423	-7.899×10^{-03}	8.003×10^{-03}	0.1507
	77	193	35.415	35.424	-8.580×10^{-03}	8.693×10^{-03}	0.1637
	79	197	36.251	36.260	-8.786×10^{-03}	8.922×10^{-03}	0.148158
	80	201	36.652	36.616	3.532×10^{-02}	-3.592×10^{-02}	-0.56023

TABLE II. *(Continued).*

I	Z	A	ΔE_0	$\Delta E_{\rm HF}$	$W(1,0)$	$W(1,1)$	μ_i
$\frac{5}{2}$	8	17	0.017	0.017	2.503×10^{-05}	-1.024×10^{-05}	-1.89379
	12	25	0.139	0.139	4.587×10^{-05}	-2.042×10^{-05}	-0.85545
	13	27	0.204	0.204	-2.556×10^{-04}	1.156×10^{-04}	3.64150687
	22	47	2.052	2.052	3.294×10^{-04}	-1.706×10^{-04}	-0.78848
	25	55	3.349	3.351	-2.264×10^{-03}	1.229×10^{-03}	3.4687190
	30	67	6.262	6.263	-1.093×10^{-03}	6.359×10^{-04}	0.8752049
	37	85	11.281	11.283	-3.595×10^{-03}	2.235×10^{-03}	1.3533515
	40	91	13.520	13.517	4.593×10^{-03}	-2.904×10^{-03}	-1.30362
	42	95	14.995	14.993	3.845×10^{-03}	-2.452×10^{-03}	-0.9142
	42	97	14.995	14.993	3.926×10^{-03}	-2.504×10^{-03}	-0.9335
	44	99	16.446	16.444	3.197×10^{-03}	-2.052×10^{-03}	-0.6413
	44	101	16.446	16.444	3.583×10^{-03}	-2.300×10^{-03}	-0.7188
	46	105	17.866	17.863	3.770×10^{-03}	-2.432×10^{-03}	-0.642
	51	121	21.262	21.281	-2.902×10^{-02}	1.888×10^{-02}	3.3634
	53	127	22.557	22.575	-2.810×10^{-02}	1.832×10^{-02}	2.813273
	59	141	26.231	26.273	-6.494×10^{-02}	4.253×10^{-02}	4.2754
	63	151	28.510	28.555	-6.881×10^{-02}	4.517×10^{-02}	3.4717
	63	153	28.510	28.530	-3.038×10^{-02}	1.995×10^{-02}	1.5330
	66	161	30.133	30.125	1.157×10^{-02}	-7.607×10^{-03}	-0.4803
	66	163	30.133	30.144	-1.620×10^{-02}	1.065×10^{-02}	0.6726
	70	173	32.179	32.165	2.112×10^{-02}	-1.392×10^{-02}	-0.67989
	75	185	34.538	34.627	-1.353×10^{-01}	8.955×10^{-02}	3.1871
	75	187	34.538	34.628	-1.367×10^{-01}	9.047×10^{-02}	3.2197
$\frac{7}{2}$	20	43	1.394	1.394	3.799×10^{-04}	-1.421×10^{-04}	-1.317643
	21	45	1.703	1.703	-1.621×10^{-03}	6.162×10^{-04}	4.7564866
	22	49	2.052	2.052	4.420×10^{-04}	-1.706×10^{-04}	-1.10417
	23	51	2.443	2.444	-2.405×10^{-03}	9.432×10^{-04}	5.14870573
	27	59	4.413	4.415	-3.800×10^{-03}	1.584×10^{-03}	4.627
	51	123	21.262	21.272	-2.109×10^{-02}	1.022×10^{-02}	2.5498
	55	133	23.816	23.830	-2.852×10^{-02}	1.388×10^{-02}	2.5829128
	57	139	25.041	25.058	-3.533×10^{-02}	1.722×10^{-02}	2.7830455
	60	143	26.813	26.805	1.658×10^{-02}	-8.100×10^{-03}	-1.065
	60	145	26.813	26.808	1.022×10^{-02}	-4.989×10^{-03}	-0.656
	62	147	27.953	27.946	1.449×10^{-02}	-7.086×10^{-03}	-0.8148
	62	149	27.953	27.947	1.194×10^{-02}	-5.841×10^{-03}	-0.6717
	67	165	30.657	30.707	-1.026×10^{-01}	5.034×10^{-02}	4.173
	68	167	31.173	31.166	1.480×10^{-02}	-7.259×10^{-03}	-0.56385
	71	175	32.669	32.704	-7.095×10^{-02}	3.488×10^{-02}	2.23799
	72	177	33.150	33.163	-2.678×10^{-02}	1.318×10^{-02}	0.7935
	73	181	33.622	33.664	-8.516×10^{-02}	4.194×10^{-02}	2.3705
	92	235	40.399	40.376	4.395×10^{-02}	-2.241×10^{-02}	-0.38
$\frac{9}{2}$	32	73	7.626	7.626	1.293×10^{-03}	-4.580×10^{-04}	-0.8794677
	36	83	10.535	10.534	2.182×10^{-03}	-8.011×10^{-04}	-0.970669
	38	87	12.028	12.027	2.989×10^{-03}	-1.112×10^{-03}	-1.0936030
	41	93	14.260	14.269	-2.222×10^{-02}	8.390×10^{-03}	6.1705
	43	99	15.724	15.734	-2.435×10^{-02}	9.262×10^{-03}	5.6847
	49	113	19.930	19.945	-3.836×10^{-02}	1.479×10^{-02}	5.5289
	49	115	19.930	19.945	-3.844×10^{-02}	1.483×10^{-02}	5.5408
	72	179	33.150	33.142	2.109×10^{-02}	-8.277×10^{-03}	-0.6409
	83	209	37.784	37.886	-2.669×10^{-01}	1.061×10^{-01}	4.1106
1	7	14	0.008	0.008	-3.939×10^{-06}	3.253×10^{-06}	0.40376100
3	5	10	0.001	0.001	-3.892×10^{-06}	1.159×10^{-06}	1.80064475
5	57	138	25.041	25.057	-4.555×10^{-02}	1.609×10^{-02}	3.713646
7	71	176	32.669	32.693	-9.472×10^{-02}	2.470×10^{-02}	3.1692
9	73	180	33.622	33.654	-1.593×10^{-01}	3.282×10^{-02}	+4.77
9	73	180[a]	33.622	33.558	1.593×10^{-01}	-3.282×10^{-02}	-4.77

[a]The sign of μ_i for ^{180}Ta is not known; therefore, calculation has been done for both signs.

TABLE III. Lifetime of the perturbed $1s^2 2s2p\ ^3P_0$ ($\tau_{0\ \mathrm{HF}}$) (the unperturbed lifetime $\tau_0 = \infty$)(in s). The lifetime of the $1s^2 2s2p\ ^3P_1$ (τ_1) is the same with or without perturbation to the decimal figures shown.

Z	A	$\tau_{0\ \mathrm{HF}}$	τ_1	Z	A	$\tau_{0\ \mathrm{HF}}$	τ_1
I=$\frac{1}{2}$							
6	13	$4.340\times10^{+03}$	1.258×10^{-02}	50	117	1.832×10^{-03}	5.960×10^{-10}
7	15	$1.056\times10^{+04}$	2.123×10^{-03}	50	119	1.673×10^{-03}	5.960×10^{-10}
9	19	$2.778\times10^{+01}$	1.610×10^{-04}	52	123	2.501×10^{-03}	5.235×10^{-10}
14	29	$4.625\times10^{+01}$	2.970×10^{-06}	52	125	1.720×10^{-03}	5.235×10^{-10}
15	31	$7.381\times10^{+00}$	1.653×10^{-06}	54	129	1.668×10^{-03}	4.640×10^{-10}
26	57	$3.059\times10^{+01}$	2.020×10^{-08}	69	169	2.306×10^{-03}	2.249×10^{-10}
34	77	1.174×10^{-01}	3.359×10^{-09}	70	171	4.450×10^{-04}	2.158×10^{-10}
39	89	6.320×10^{-01}	1.619×10^{-09}	74	183	4.523×10^{-03}	1.839×10^{-10}
45	103	5.234×10^{-01}	8.725×10^{-10}	76	187	1.140×10^{-02}	1.701×10^{-10}
47	107	2.284×10^{-01}	7.408×10^{-10}	78	195	9.803×10^{-05}	1.577×10^{-10}
47	109	1.729×10^{-01}	7.408×10^{-10}	80	199	1.082×10^{-04}	1.467×10^{-10}
48	111	7.092×10^{-03}	6.867×10^{-10}	81	203	9.276×10^{-06}	1.415×10^{-10}
48	113	6.481×10^{-03}	6.867×10^{-10}	81	205	9.098×10^{-06}	1.415×10^{-10}
50	115	2.175×10^{-03}	5.960×10^{-10}	82	207	5.992×10^{-05}	1.366×10^{-10}
I=$\frac{3}{2}$							
5	11	$1.567\times10^{+03}$	1.417×10^{-01}	33	75	3.658×10^{-02}	4.011×10^{-09}
10	21	$4.226\times10^{+02}$	5.921×10^{-05}	35	79	1.095×10^{-02}	2.846×10^{-09}
11	23	$2.161\times10^{+01}$	2.468×10^{-05}	35	81	9.423×10^{-03}	2.846×10^{-09}
16	33	$2.769\times10^{+01}$	9.617×10^{-07}	54	131	3.807×10^{-03}	4.640×10^{-10}
17	35	$1.169\times10^{+01}$	5.813×10^{-07}	56	135	1.940×10^{-03}	4.146×10^{-10}
17	37	$1.686\times10^{+01}$	5.813×10^{-07}	56	137	1.551×10^{-03}	4.146×10^{-10}
19	39	$2.543\times10^{+01}$	2.338×10^{-07}	64	155	6.692×10^{-03}	2.794×10^{-10}
19	41	$8.439\times10^{+01}$	2.338×10^{-07}	64	157	3.892×10^{-03}	2.794×10^{-10}
24	53	$3.555\times10^{+00}$	3.687×10^{-08}	65	159	9.543×10^{-05}	2.672×10^{-10}
28	61	4.634×10^{-01}	1.182×10^{-08}	76	189	1.972×10^{-04}	1.701×10^{-10}
29	63	4.049×10^{-02}	9.261×10^{-09}	77	191	3.294×10^{-03}	1.638×10^{-10}
29	65	3.542×10^{-02}	9.261×10^{-09}	77	193	2.792×10^{-03}	1.638×10^{-10}
31	69	2.991×10^{-02}	5.933×10^{-09}	79	197	2.589×10^{-03}	1.520×10^{-10}
31	71	1.853×10^{-02}	5.933×10^{-09}	80	201	1.576×10^{-04}	1.467×10^{-10}
I=$\frac{5}{2}$							
8	17	$2.280\times10^{+02}$	5.185×10^{-04}	46	105	1.801×10^{-02}	8.023×10^{-10}
12	25	$1.036\times10^{+02}$	1.133×10^{-05}	51	121	2.999×10^{-04}	5.578×10^{-10}
13	27	$3.582\times10^{+00}$	5.622×10^{-06}	53	127	3.176×10^{-04}	4.922×10^{-10}
22	47	$2.812\times10^{+00}$	7.244×10^{-08}	59	141	5.799×10^{-05}	3.543×10^{-10}
25	55	5.924×10^{-02}	2.705×10^{-08}	63	151	5.036×10^{-05}	2.924×10^{-10}
30	67	2.419×10^{-01}	7.361×10^{-09}	63	153	2.578×10^{-04}	2.924×10^{-10}
37	85	2.076×10^{-02}	2.107×10^{-09}	66	161	1.732×10^{-03}	2.555×10^{-10}
40	91	1.245×10^{-02}	1.437×10^{-09}	66	163	8.844×10^{-04}	2.555×10^{-10}
42	95	1.758×10^{-02}	1.156×10^{-09}	70	173	5.007×10^{-04}	2.158×10^{-10}
42	97	1.686×10^{-02}	1.156×10^{-09}	75	185	1.158×10^{-05}	1.767×10^{-10}
44	99	2.522×10^{-02}	9.534×10^{-10}	75	187	1.135×10^{-05}	1.767×10^{-10}
44	101	2.008×10^{-02}	9.534×10^{-10}				
I=$\frac{7}{2}$							
20	43	$2.081\times10^{+00}$	1.545×10^{-07}	60	145	2.322×10^{-03}	3.371×10^{-10}
21	45	1.155×10^{-01}	1.046×10^{-07}	62	147	1.140×10^{-03}	3.064×10^{-10}
22	49	$1.562\times10^{+00}$	7.244×10^{-08}	62	149	1.678×10^{-03}	3.064×10^{-10}
23	51	5.286×10^{-02}	5.118×10^{-08}	67	165	2.194×10^{-05}	2.450×10^{-10}
27	59	2.069×10^{-02}	1.533×10^{-08}	68	167	1.040×10^{-03}	2.344×10^{-10}
51	123	5.677×10^{-04}	5.578×10^{-10}	71	175	4.400×10^{-05}	2.071×10^{-10}
55	133	3.059×10^{-04}	4.382×10^{-10}	72	177	3.052×10^{-04}	1.990×10^{-10}
57	139	1.976×10^{-04}	3.928×10^{-10}	73	181	2.986×10^{-05}	1.911×10^{-10}
60	143	8.806×10^{-04}	3.371×10^{-10}	92	235	8.562×10^{-05}	1.014×10^{-10}
I=$\frac{9}{2}$							
32	73	1.685×10^{-01}	4.847×10^{-09}	49	113	1.727×10^{-04}	6.387×10^{-10}
36	83	5.679×10^{-02}	2.437×10^{-09}	49	115	1.720×10^{-04}	6.387×10^{-10}
38	87	2.977×10^{-02}	1.839×10^{-09}	72	179	4.915×10^{-04}	1.990×10^{-10}
41	93	5.298×10^{-04}	1.285×10^{-09}	83	209	2.661×10^{-06}	1.320×10^{-10}
43	99	4.372×10^{-04}	1.047×10^{-09}				

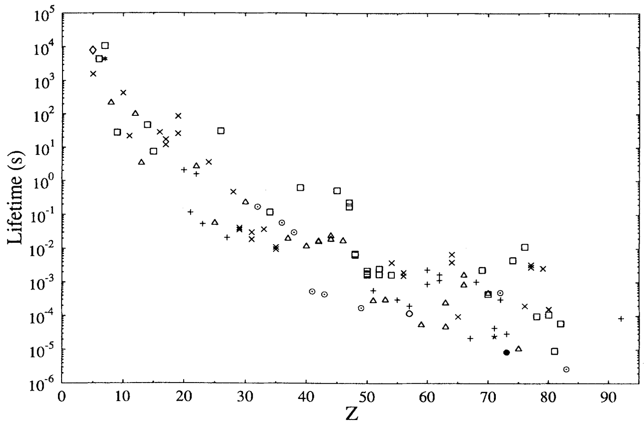

FIG. 3. Influence of the hyperfine interaction on the lifetime of the $1s^22s2p\ ^3P_0$ state, as a function of Z (the unperturbed lifetime is infinite). The symbols □, ×, △, +, ⊙, *, ◇, ○, ⋆, and • represent $\tau_{0\ \mathrm{HF}}$ for isotope with nuclear spin I of $\frac{1}{2}$, $\frac{3}{2}$, $\frac{5}{2}$, $\frac{7}{2}$, $\frac{9}{2}$, 1, 3, 5, 7, and 9, respectively.

10^{-7} s^{-1}. In contrast the hyperfine-quenched transition rate for ^{207}Pb is 1.7×10^4 s^{-1}, i.e., 11 orders of magnitude larger. This is very different from the heliumlike case, because here the $1s^22s2p\ ^3P_0$–$1s^22s^2\ ^1S_0$ transition energy is of a few hundred eV at $Z = 82$, while the $1s2p\ ^3P_0$–$1s^2\ ^1S_0$ transition energy is ≈ 70 keV for the corresponding heliumlike ion.

One of the most interesting practical implications of these calculations is due to the relation between the $1s^22s2p\ ^3P_0 - 1s^22s2p\ ^3P_1$ energy separation and the $1s^22s2p\ ^3P_0$ lifetime [Eq. (2.6)]. As in the heliumlike case, this energy separation is not easy to measure directly in spectroscopy. The perturbed energy is not easily measured either. It is mostly the sum of the unperturbed energy and of $W(1,1)$, and $W(1,0)$ does not play any role in its value. The $1s^22s2p\ ^3P_0$ lifetime in contrast is very sensitive to both the separation energy ΔE_0 and $W(1,0)$.

It could thus be possible to estimate ΔE_0 through a

TABLE III. *(Continued).*

I	Z	A	$\tau_{0\ \mathrm{HF}}$	τ_1
3	5	10	$4.340\times10^{+03}$	1.417×10^{-01}
1	7	14	$7.806\times10^{+03}$	2.123×10^{-03}
5	57	138	1.189×10^{-04}	3.928×10^{-10}
7	71	176	2.467×10^{-05}	2.071×10^{-10}
9	73	180	8.530×10^{-06}	1.911×10^{-10}
9	73	180[a]	8.496×10^{-06}	1.911×10^{-10}

[a]The sign of μ_i for ^{180}Ta is not known; therefore, calculation has been done for both signs.

measurement of the hyperfine-quenched $1s^22s2p\ ^3P_0$ lifetime of berylliumlike ions with nuclear spin $I \neq 0$. The method has been demonstrated in heliumlike Ag^{45+} [2] and Gd^{62+} [3]. The berylliumlike ions case is rather different, because, even for the highest Z the lifetimes involved are much longer than in heavy heliumlike ions. However, because of recent progress in ion sources and ion trap technology, lifetimes between 0.1 s and 10 μs could be measured with some accuracy, by directly looking at the light emitted by the ions as a function of time, after the trap has been loaded. Obviously it means that the vacuum inside the trap has to be very good if long lifetimes have to be measured. Whether this method will work remains to be experimentally demonstrated. But such experiments would provide for different isotopes, the unperturbed energy separation, since nuclear magnetic moments are well known. This would be a very interesting test of our relativistic calculations.

ACKNOWLEDGMENTS

The MCDF calculations presented in this work have been done using the computer facilities at the Centro de Física Atómica da Universidade de Lisboa (INIC) and at the LPAN, Laboratoire the Physique Atomique et Nucléaire. LPAN is "Unité de Recherche Associée au CNRS No. 771."

[1] P. Indelicato, F. Parente, and R. Marrus, Phys. Rev. A **40**, 3505 (1989).
[2] R. Marrus, A. Simionovici, P. Indelicato, D. D. Dietrich, P. Charles, J. P. Briand, K. Finlayson, F. Bosch, D. Liesen, and F. Parente, Phys. Rev. Lett. **63**, 502 (1989).
[3] P. Indelicato, B. B. Birkett, J. P. Briand, P. Charles, D. D. Dietrich, R. Marrus, and A. Simionovici, Phys. Rev. Lett. **68**, 1307 (1992).
[4] W. R. Johnson and C. D. Lin, Phys. Rev. A **14**, 565 (1976).
[5] K. T. Cheng and W. J. Childs, Phys. Rev. A **31**, 2775 (1985).
[6] O. Gorceix, P. Indelicato, and J. P. Desclaux, J. Phys. B **20**, 639 (1987).
[7] P. Indelicato, O. Gorceix, and J. P. Desclaux, J. Phys. B **20**, 651 (1987).
[8] P. Indelicato, Nucl. Instrum. Methods Phys. Res. Sect. B **31**, 14 (1988).
[9] E. Lindroth and J. Hvarfner, Phys. Rev. A **45**, 2771 (1992).
[10] I. Lindgren, J. Phys. B **23**, 1085 (1990).
[11] P. Raghavan, At. Data Nucl. Data Tables **42**, 189 (1989).